

Received April 9, 2020, accepted April 24, 2020, date of publication April 28, 2020, date of current version May 13, 2020.

Digital Object Identifier 10.1109/ACCESS.2020.2991089

Cost Effective Offline Reconfiguration for Large-Scale Non-Uniformly Aging Photovoltaic Arrays Efficiency Enhancement

ZUYU WU^{ID1}, CHEN ZHANG², MOHAMMED ALKAHTANI^{ID3}, YIHUA HU^{ID1}, (Senior Member, IEEE), AND JIANGFENG ZHANG^{ID4}

¹Department of Electrical and Engineering, University of York, York YO10 5DD, U.K.

²School of Electrical and Power Engineering, China University of Mining and Technology, Xuzhou 221116, China

³Department of Electrical and Engineering, University of Liverpool, Liverpool L69 3GJ, U.K.

⁴Department of Automotive Engineering, Clemson University, Greenville, SC 29607, USA

Corresponding author: Chen Zhang (zc@cumt.edu.cn)

ABSTRACT In the past decades, a huge number of large-scale photovoltaic (PV) plants have been constructed all around the world. However, the capital and operational costs can be high, which limits their widespread applications. Because the installed PV modules often operate in harsh environments (i.e. storm, high temperature, dust, hail, etc.), non-uniform aging phenomena of PV modules cannot be avoided and it impacts adversely on the performance of PV plants, especially in the middle and late periods of their service life. This paper develops an offline PV module reconfiguration strategy for the non-uniform aging PV array to mitigate this effect. In order to maximize the economic benefit, electricity price and labor cost are considered in the offline reconfiguration. The Branch-and-Bound based optimization algorithm is proposed to find the highest economic benefit. In order to verify the proposed algorithm, MATLAB software-based modelling and simulation have been performed in four case studies, in which a typical 42kW PV array with 7×20 connection is employed in a testing benchmark, and the manpower cost and electricity price in USA, UK, China and Turkey are considered in the case study. The results demonstrate that the economic benefit from a non-uniformly aged PV array is further enhanced with the proposed reconfiguration method.

INDEX TERMS Maximum power tracking, non-uniform aging, offline reconfiguration, output characteristics, photovoltaics, solar energy.

I. INTRODUCTION

Thanks to the decrease in cost, solar energy generation is becoming popular all around the world over the years [1]–[6]. Currently, large-scale PV power plants are gaining popularity in the global renewable energy market, primarily owing to the mass production of PV modules with reduced cost and high energy conversion efficiency [7], [8].

There are three factors that determine the PV generation system efficiency. They are the PV cell efficiency, PV array efficiency and energy conversion efficiency. PV cell and energy conversion have been widely studied to improve the efficiency. With the improvement of technology, monocrystalline silicon and polycrystalline silicon production cost is decreased obviously. Currently, the typical polycrystalline

The associate editor coordinating the review of this manuscript and approving it for publication was Huiqing Wen^{ID}.

silicon PV cell efficiency is 17.7% (Yinli Solar); the monocrystalline silicon PV cell efficiency is 19.8% (Yinli Solar) [9]. In energy conversion, a new generation of switching devices such as super junction MOSFET, silicon carbon (SiC) MOSFET, and new power electronics topologies such multi-level DC-AC converter, resonant DC-DC converter have obviously improved the energy conversion efficiency [10]–[12]. Due to the soft switching topology and high-quality switching devices, the energy conversion can be over 95% [12]. Therefore, there is limited space in improving efficiencies in PV cell and energy conversion. However, there is large room for improving the PV array efficiency.

The non-uniform aging of PV array is a common phenomenon in the long service time, which is caused by dust, shadow, and water corrosion [13], [14]. Figure 1 is an example of aging improvement and global maximum power point (GMPPT). For aging improvement, changing PV modules

position is needed according to aging information. After rearrangement, the PV array output characteristic may still be with multi-maximum power points. GMPPT is the necessary algorithm that find the global maximum power point. We can see from Figure 1 that before rearrangement the array GMPPT is 564 W, after rearrangement the array GMPPT is 690 W. The whole array efficiency can be improved by 22.3% when the working point of the array is the GMPPT. Therefore, the proposed aging array rearrangement is complementary with GMPPT.

To increase the effective service time, there are two important steps. The first step is PV array fault diagnosis; the second step is PV array reconfiguration. For PV array fault diagnosis, thermal camera [16]–[21], earth capacitance measurement (ECM) [22], time domain reflectometry (TDR) [23], and applying voltage/current sensors are four popular methods for PV fault diagnosis. Due to the non-uniform temperature distribution of faulty PV array, the thermal camera can be adapted to locate faulty PV module in online application background [16]–[21]. ECM can locate the disconnection of PV modules; and TDR can estimate the degradation of PV arrays; while both ECM and TDR can only be employed in offline fault diagnosis [22], [23]. For scale PV array fault diagnosis, power loss analysis is proposed in [24], [25]. For PV array reconfiguration, [26]–[29] only give the small-scale reconfiguration example. Paper [30] proposed a classical optimization algorithm (COA) to reconfigure a reconfigurable total cross-tied (RTCT) arrays. The branch-and-bound algorithm is employed to minimize the cost, while the COA still needs a strong computational effort. The look-up table method is developed in paper [28] in small-scale PV arrays, which is almost impossible to use for large PV arrays. Paper [31] developed an exhaustive search algorithm. In order to speed up the selection of a configuration, paper [32] developed a sorting algorithm based on the best-worst paradigm. The fuzzy logical algorithm also proposed to search for the best reconfiguration [33]. Paper [34] gives the summary of the state-of-art online reconfiguration of PV array.

However, there is no report on large-scale PV array reconfiguration. Currently, PV array reconfiguration is mainly implemented by relay networks, which needs a large number of relays and high system cost. For large-scale PV arrays, the only feasible solution for PV reconfiguration is swapping PV modules by human labor offline, as shown in Figure 2. In order to decrease the labor cost, the key technology is to develop an optimized reconfiguration strategy to decrease the swap times and achieve the maximum power at the same time. In this paper, the optimized reconfiguration strategy with the minimum swap times and maximum output power is proposed to decrease the labor cost.

In this paper, in section II, four levels model including cell-unit, PV module, PV string and PV array are introduced. In section III, two physical methods are illustrated. In section IV, the lost cost PV array rearrangement strategy is developed. In section V, simulation and experiment are

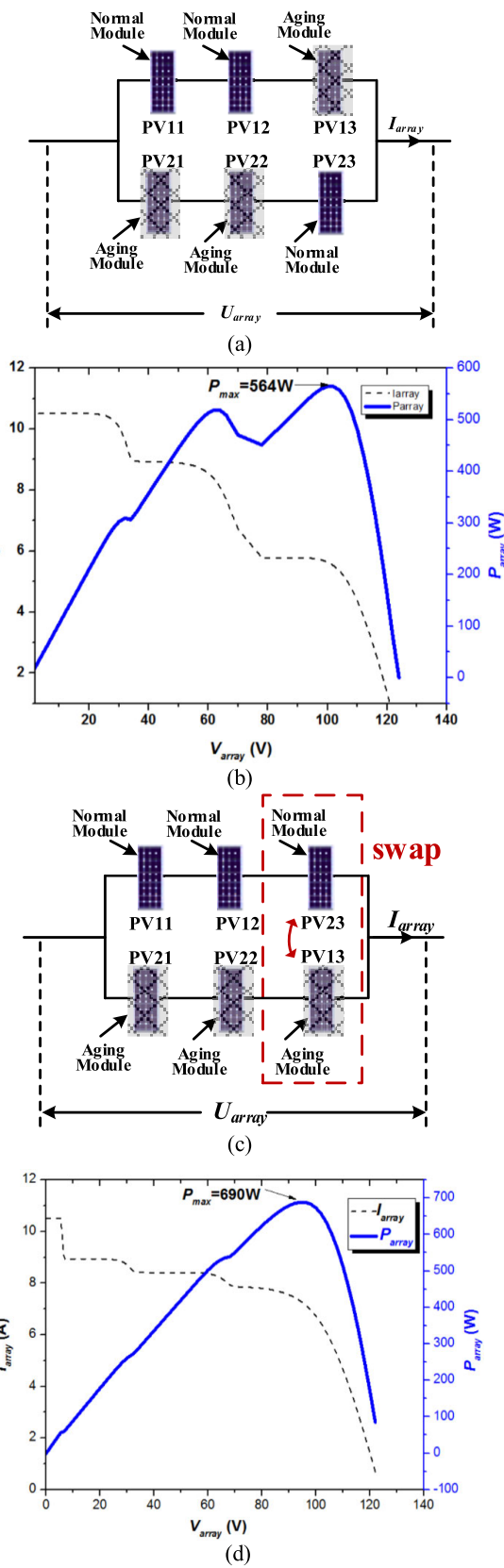
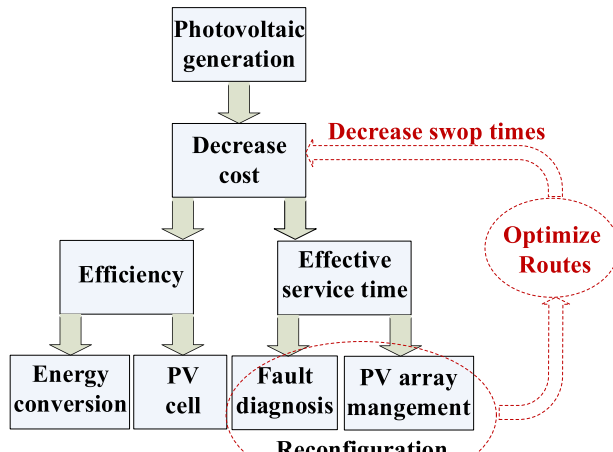
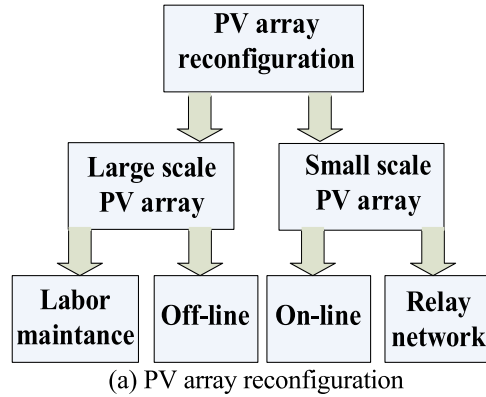


FIGURE 1. Without and with rearrangement. (a) without rearrangement (b) Output character (Without) (c) with rearrangement (d) Output character (With).



presented to verify the proposed method. Conclusions are given in the final part.

II. MATHEMATICAL MODELING

Non-uniform aging is a common problem in PVs which can be caused by lasting dust, shading, or water corrosion over a long time [13], [14].

The electrical characteristics of PVs are influenced by both temperature and illumination. The electrical model of the PV cell is expressed by [2].

$$I = I_L - I_o \left[\exp\left(\frac{\varepsilon \cdot V}{T_m}\right) - 1 \right] \quad (1)$$

$$\varepsilon = \frac{q}{N_s \cdot K \cdot A} \quad (2)$$

$$I_L = \frac{G}{G_{ref}} [I_{Lref} + k_i(T_m - T_{ref})] \quad (3)$$

$$I_o = I_{oref} \left(\frac{T_m}{T_{ref}} \right)^3 \exp\left[\frac{q \cdot E_{BG}}{N_s \cdot A \cdot K} \left(\frac{1}{T_{ref}} - \frac{1}{T_m} \right)\right] \quad (4)$$

where I is the PV module output current, I_L is the photon current, q is the quantity of electric charge, A is the diode characteristic factor, K is the Boltzmann constant, I_o is the saturated current, T_m is the PV module temperature, G is

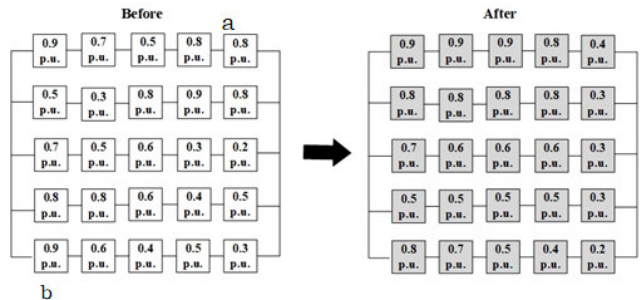


FIGURE 3. Schematic diagram of PV module replacement.

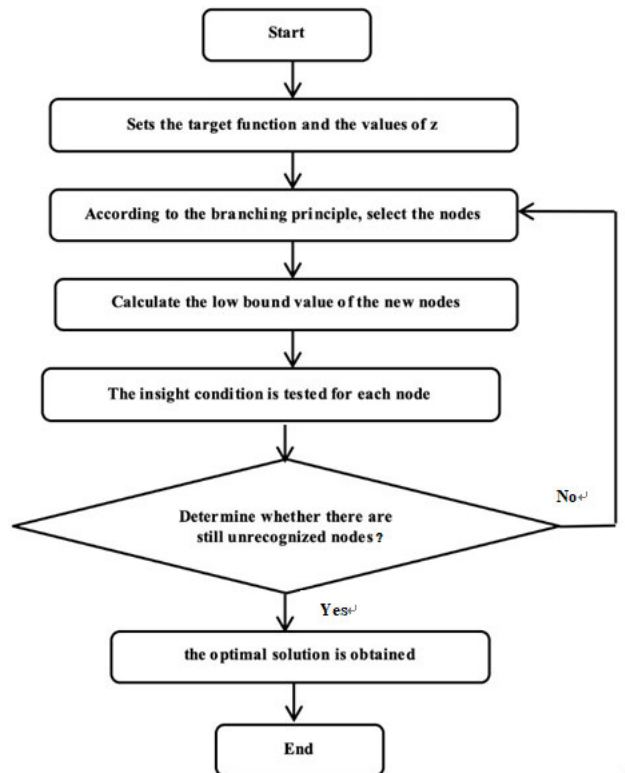


FIGURE 4. Flowchart of the proposed algorithm.

the irradiance, V is the output voltage, G_{ref} is the reference irradiance level (1000 W/m^2), I_{Lref} , I_{oref} are the reference values for I_L and I_o . k_i is the current-temperature coefficient provided by the PV manufacturer. T_{ref} is the reference temperature, N_s is the number of series-connected cells, T_m is the PV module temperature. ε is a constant depending on q , N_s , K , A , and is calculated by the following equation:

$$I_{sc_ref} - I_{mpp_ref} = \frac{I_{sc_ref}}{\exp\left(\frac{\varepsilon \cdot V_{oc_ref}}{T_{ref}}\right) - 1} \left[\exp\left(\frac{\varepsilon \cdot V_{mpp_ref}}{T_{ref}}\right) - 1 \right] \quad (5)$$

where I_{mpp_ref} , I_{sc_ref} , V_{mpp_ref} and V_{oc_ref} are the maximum power point (MPP) current, short-circuit current,

TABLE 1. Electricity price and labor remuneration in 2019.

Country	Electricity prices (\$/ KWH)	The average salary (\$/ hour)	handling cost per swapping (\$/time)
China [1]	0.084	7.4	5.55
America	0.125	16	12
Britain	0.256	17.2	12.9
Turkey	0.17	3.01	2.26

MPP voltage and open-circuit voltage at a reference condition defined by the relevant standard.

A PV string consists of s PV modules, with the terminal voltage V_{string} and current i_{string} . Let the terminal voltage, current and maximum current from the k th PV module be $V_{module,k}$, $i_{module,k}$ and $i_{module,k}^{max}$, respectively. The following relationship can be established.

$$i_{string} = i_{module,1} = i_{module,2} = \dots = i_{module,s} \quad (6)$$

$$V_{string} = V_{module,1} + V_{module,2} + \dots + V_{module,s} \quad (7)$$

Similarly, the bucket effect indicates that the maximum current in the PV string is limited by the minimum $i_{module,k}^{max}$.

of those non-bypassed modules. That is $i_{string} \leq i_{module,k}^{max}$, $1 \leq k \leq s$, and the k th module is not bypassed.

In order to calculate the number of reconfigured PV panels T_{st} , the following notations are needed. Assume that the original PV array has m rows of PV panels connected in parallel, and each row has n panels connected in series. Define the reconfiguration function $f(k)$ for $k = 1, 2, \dots, m * n$, so that the value of $f(k)$ equals an integer from $\{1, 2, \dots, m * n\}$, and it represents the correspondence between the original PV array and the reconfigured PV array. For instance, for any PV module located in the i -th row and j -th column, then this module corresponds to a number $k = i * n + j$, then this module will be moved to the location of i' -th row and j' -th column, where are determined from the relation $f(k) = i' * n + j'$ that is, $j' = f(k) \bmod (n)$, $i' = \frac{f(k)-j'}{n}$.

In the calculation process of T_{st} , it is crucial to note that the movement of a panel within one row is not counted as a movement, since all modules in the same row are connected in series. It is also helpful to note that swapping two rows is not indeed a movement, as such a swap does not change the topological structure—this case usually scarcely happens. Keep this in mind, and T_{st} can be calculated as follows.

$$T_{st} = \min\{T_{st}^l : l = 1, 2, 3, \dots, m!\} \quad (8)$$

where T_{st}^l is the number of reconfigured PV panels under the l -th permutation of these rows of the reconfigured solution.

TABLE 2. PV array before arrangement for second case in China.

Before																				
0.7	0.8	0.7	0.5	0.4	0.8	0.5	0.7	0.4	0.4	0.7	0.8	0.7	0.5	0.4	0.8	0.5	0.7	0.4	0.3	
p.u.	p.u.	p.u.	p.u.	p.u.	p.u.	p.u.	p.u.	p.u.	p.u.	p.u.	p.u.	p.u.	p.u.	p.u.	p.u.	p.u.	p.u.	p.u.	p.u.	
0.6	0.7	0.6	0.7	0.7	0.7	0.4	0.7	0.6	0.6	0.6	0.7	0.6	0.7	0.7	0.7	0.7	0.4	0.7	0.6	0.6
p.u.	p.u.	p.u.	p.u.	p.u.	p.u.	p.u.	p.u.	p.u.	p.u.	p.u.	p.u.	p.u.	p.u.	p.u.	p.u.	p.u.	p.u.	p.u.	p.u.	
0.7	0.7	0.7	0.8	0.6	0.6	0.8	0.5	0.7	0.6	0.7	0.7	0.7	0.8	0.6	0.6	0.8	0.5	0.7	0.6	0.6
p.u.	p.u.	p.u.	p.u.	p.u.	p.u.	p.u.	p.u.	p.u.	p.u.	p.u.	p.u.	p.u.	p.u.	p.u.	p.u.	p.u.	p.u.	p.u.	p.u.	
0.8	0.6	0.7	0.7	0.6	0.7	0.7	0.8	0.5	0.5	0.8	0.6	0.7	0.7	0.7	0.7	0.7	0.7	0.8	0.5	0.7
p.u.	p.u.	p.u.	p.u.	p.u.	p.u.	p.u.	p.u.	p.u.	p.u.	p.u.	p.u.	p.u.	p.u.	p.u.	p.u.	p.u.	p.u.	p.u.	p.u.	
0.8	0.6	0.7	0.7	0.6	0.7	0.7	0.8	0.5	0.5	0.8	0.6	0.7	0.7	0.7	0.7	0.7	0.7	0.8	0.5	0.7
p.u.	p.u.	p.u.	p.u.	p.u.	p.u.	p.u.	p.u.	p.u.	p.u.	p.u.	p.u.	p.u.	p.u.	p.u.	p.u.	p.u.	p.u.	p.u.	p.u.	
0.8	0.8	0.8	0.6	0.5	0.5	0.7	0.5	0.6	0.5	0.8	0.8	0.7	0.6	0.5	0.5	0.7	0.5	0.6	0.5	0.5
p.u.	p.u.	p.u.	p.u.	p.u.	p.u.	p.u.	p.u.	p.u.	p.u.	p.u.	p.u.	p.u.	p.u.	p.u.	p.u.	p.u.	p.u.	p.u.	p.u.	
0.8	0.8	0.8	0.6	0.5	0.5	0.7	0.5	0.6	0.5	0.8	0.8	0.7	0.6	0.5	0.5	0.7	0.5	0.6	0.5	0.5
p.u.	p.u.	p.u.	p.u.	p.u.	p.u.	p.u.	p.u.	p.u.	p.u.	p.u.	p.u.	p.u.	p.u.	p.u.	p.u.	p.u.	p.u.	p.u.	p.u.	
0.7	0.9	0.8	0.7	0.6	0.5	0.6	0.9	0.7	0.5	0.7	0.9	0.8	0.7	0.6	0.5	0.6	0.9	0.7	0.5	0.5
p.u.	p.u.	p.u.	p.u.	p.u.	p.u.	p.u.	p.u.	p.u.	p.u.	p.u.	p.u.	p.u.	p.u.	p.u.	p.u.	p.u.	p.u.	p.u.	p.u.	
0.9	0.9	0.8	0.7	0.6	0.6	0.6	0.9	0.7	0.9	0.7	0.8	0.8	0.7	0.9	0.6	0.6	0.9	0.8	0.7	0.7
p.u.	p.u.	p.u.	p.u.	p.u.	p.u.	p.u.	p.u.	p.u.	p.u.	p.u.	p.u.	p.u.	p.u.	p.u.	p.u.	p.u.	p.u.	p.u.	p.u.	
After																				
0.7	0.8	0.6	0.5	0.5	0.5	0.5	0.5	0.5	0.5	0.5	0.5	0.5	0.5	0.5	0.5	0.5	0.5	0.4	0.3	
p.u.	p.u.	p.u.	p.u.	p.u.	p.u.	p.u.	p.u.	p.u.	p.u.	p.u.	p.u.	p.u.	p.u.	p.u.	p.u.	p.u.	p.u.	p.u.	p.u.	
0.6	0.7	0.6	0.7	0.7	0.7	0.6	0.7	0.6	0.6	0.7	0.6	0.6	0.7	0.6	0.4	0.4	0.6	0.6	0.6	0.6
p.u.	p.u.	p.u.	p.u.	p.u.	p.u.	p.u.	p.u.	p.u.	p.u.	p.u.	p.u.	p.u.	p.u.	p.u.	p.u.	p.u.	p.u.	p.u.	p.u.	
0.7	0.7	0.7	0.8	0.7	0.7	0.7	0.8	0.7	0.7	0.8	0.7	0.7	0.7	0.7	0.7	0.7	0.7	0.5	0.5	0.5
p.u.	p.u.	p.u.	p.u.	p.u.	p.u.	p.u.	p.u.	p.u.	p.u.	p.u.	p.u.	p.u.	p.u.	p.u.	p.u.	p.u.	p.u.	p.u.	p.u.	
0.7	0.7	0.7	0.7	0.7	0.7	0.7	0.7	0.7	0.7	0.7	0.7	0.7	0.7	0.7	0.7	0.7	0.7	0.7	0.5	0.4
p.u.	p.u.	p.u.	p.u.	p.u.	p.u.	p.u.	p.u.	p.u.	p.u.	p.u.	p.u.	p.u.	p.u.	p.u.	p.u.	p.u.	p.u.	p.u.	p.u.	
0.6	0.7	0.6	0.6	0.9	0.7	0.8	0.7	0.7	0.8	0.8	0.8	0.8	0.8	0.8	0.8	0.7	0.8	0.7	0.5	0.5
p.u.	p.u.	p.u.	p.u.	p.u.	p.u.	p.u.	p.u.	p.u.	p.u.	p.u.	p.u.	p.u.	p.u.	p.u.	p.u.	p.u.	p.u.	p.u.	p.u.	
0.6	0.6	0.8	0.6	0.6	0.6	0.7	0.6	0.6	0.6	0.6	0.6	0.6	0.6	0.6	0.6	0.6	0.6	0.6	0.5	0.4
p.u.	p.u.	p.u.	p.u.	p.u.	p.u.	p.u.	p.u.	p.u.	p.u.	p.u.	p.u.	p.u.	p.u.	p.u.	p.u.	p.u.	p.u.	p.u.	p.u.	
0.9	0.9	0.8	0.5	0.9	0.9	0.9	0.9	0.9	0.9	0.9	0.9	0.9	0.9	0.9	0.9	0.9	0.9	0.8	0.8	0.4
p.u.	p.u.	p.u.	p.u.	p.u.	p.u.	p.u.	p.u.	p.u.	p.u.	p.u.	p.u.	p.u.	p.u.	p.u.	p.u.	p.u.	p.u.	p.u.	p.u.	

TABLE 3. PV array before arrangement for second case in USA.

Before																								
0.7	0.8	0.7	0.5	0.4	0.8	0.5	0.7	0.4	0.4	0.7	0.8	0.7	0.5	0.4	0.8	0.5	0.7	0.4	0.4	0.3	p.u.	p.u.		
0.6	0.7	0.6	0.7	0.7	0.7	0.4	0.7	0.6	0.6	0.6	0.7	0.6	0.7	0.7	0.7	0.7	0.4	0.7	0.6	0.6	p.u.	p.u.		
p.u.	p.u.	p.u.	p.u.	p.u.	p.u.	p.u.	p.u.	p.u.	p.u.	p.u.	p.u.	p.u.	p.u.	p.u.	p.u.	p.u.	p.u.	p.u.	p.u.	p.u.	p.u.	p.u.	p.u.	
0.7	0.7	0.7	0.8	0.6	0.6	0.8	0.5	0.7	0.6	0.7	0.7	0.7	0.8	0.6	0.6	0.8	0.5	0.7	0.6	0.6	p.u.	p.u.		
p.u.	p.u.	p.u.	p.u.	p.u.	p.u.	p.u.	p.u.	p.u.	p.u.	p.u.	p.u.	p.u.	p.u.	p.u.	p.u.	p.u.	p.u.	p.u.	p.u.	p.u.	p.u.	p.u.	p.u.	
0.8	0.6	0.7	0.7	0.6	0.7	0.7	0.8	0.5	0.5	0.8	0.6	0.6	0.7	0.7	0.7	0.7	0.7	0.7	0.8	0.5	0.7	0.6	0.7	
p.u.	p.u.	p.u.	p.u.	p.u.	p.u.	p.u.	p.u.	p.u.	p.u.	p.u.	p.u.	p.u.	p.u.	p.u.	p.u.	p.u.	p.u.	p.u.	p.u.	p.u.	p.u.	p.u.	p.u.	
0.8	0.8	0.8	0.6	0.5	0.5	0.7	0.5	0.6	0.5	0.8	0.8	0.7	0.6	0.5	0.5	0.7	0.5	0.6	0.5	0.5	0.6	0.5	0.5	
p.u.	p.u.	p.u.	p.u.	p.u.	p.u.	p.u.	p.u.	p.u.	p.u.	p.u.	p.u.	p.u.	p.u.	p.u.	p.u.	p.u.	p.u.	p.u.	p.u.	p.u.	p.u.	p.u.	p.u.	
0.7	0.9	0.8	0.7	0.6	0.5	0.6	0.9	0.7	0.5	0.7	0.9	0.8	0.7	0.6	0.5	0.6	0.9	0.7	0.5	0.9	0.7	0.5	0.5	
p.u.	p.u.	p.u.	p.u.	p.u.	p.u.	p.u.	p.u.	p.u.	p.u.	p.u.	p.u.	p.u.	p.u.	p.u.	p.u.	p.u.	p.u.	p.u.	p.u.	p.u.	p.u.	p.u.	p.u.	
0.9	0.9	0.8	0.7	0.6	0.6	0.6	0.9	0.7	0.9	0.7	0.8	0.8	0.7	0.9	0.6	0.6	0.9	0.8	0.9	0.8	0.7	0.9	0.7	
p.u.	p.u.	p.u.	p.u.	p.u.	p.u.	p.u.	p.u.	p.u.	p.u.	p.u.	p.u.	p.u.	p.u.	p.u.	p.u.	p.u.	p.u.	p.u.	p.u.	p.u.	p.u.	p.u.	p.u.	
After																								
0.6	0.5	0.8	0.4	0.4	0.5	0.5	0.5	0.5	0.5	0.5	0.5	0.5	0.5	0.5	0.5	0.5	0.5	0.5	0.5	0.4	0.3	p.u.	p.u.	
0.6	0.7	0.6	0.9	0.7	0.7	0.4	0.8	0.8	0.8	0.8	0.8	0.8	0.8	0.8	0.8	0.8	0.7	0.7	0.8	0.5	0.5	p.u.	p.u.	
p.u.	p.u.	p.u.	p.u.	p.u.	p.u.	p.u.	p.u.	p.u.	p.u.	p.u.	p.u.	p.u.	p.u.	p.u.	p.u.	p.u.	p.u.	p.u.	p.u.	p.u.	p.u.	p.u.	p.u.	
0.7	0.7	0.7	0.7	0.7	0.7	0.7	0.7	0.7	0.7	0.7	0.7	0.7	0.7	0.7	0.7	0.7	0.7	0.7	0.7	0.7	0.5	0.4	0.4	
p.u.	p.u.	p.u.	p.u.	p.u.	p.u.	p.u.	p.u.	p.u.	p.u.	p.u.	p.u.	p.u.	p.u.	p.u.	p.u.	p.u.	p.u.	p.u.	p.u.	p.u.	p.u.	p.u.	p.u.	
0.8	0.8	0.8	0.7	0.7	0.7	0.7	0.7	0.7	0.7	0.7	0.7	0.7	0.7	0.7	0.7	0.7	0.7	0.7	0.7	0.7	0.5	0.5	0.5	
p.u.	p.u.	p.u.	p.u.	p.u.	p.u.	p.u.	p.u.	p.u.	p.u.	p.u.	p.u.	p.u.	p.u.	p.u.	p.u.	p.u.	p.u.	p.u.	p.u.	p.u.	p.u.	p.u.	p.u.	
0.7	0.7	0.7	0.7	0.7	0.7	0.7	0.7	0.7	0.7	0.6	0.6	0.6	0.6	0.6	0.6	0.6	0.6	0.6	0.6	0.6	0.5	0.4	0.4	
p.u.	p.u.	p.u.	p.u.	p.u.	p.u.	p.u.	p.u.	p.u.	p.u.	p.u.	p.u.	p.u.	p.u.	p.u.	p.u.	p.u.	p.u.	p.u.	p.u.	p.u.	p.u.	p.u.	p.u.	
0.7	0.6	0.8	0.6	0.6	0.6	0.6	0.6	0.6	0.6	0.6	0.6	0.6	0.6	0.6	0.6	0.6	0.6	0.6	0.6	0.6	0.4	0.5	0.5	
p.u.	p.u.	p.u.	p.u.	p.u.	p.u.	p.u.	p.u.	p.u.	p.u.	p.u.	p.u.	p.u.	p.u.	p.u.	p.u.	p.u.	p.u.	p.u.	p.u.	p.u.	p.u.	p.u.	p.u.	
0.9	0.9	0.8	0.8	0.6	0.9	0.9	0.9	0.9	0.9	0.8	0.8	0.8	0.8	0.9	0.8	0.8	0.9	0.8	0.9	0.8	0.5	0.5	0.5	
p.u.	p.u.	p.u.	p.u.	p.u.	p.u.	p.u.	p.u.	p.u.	p.u.	p.u.	p.u.	p.u.	p.u.	p.u.	p.u.	p.u.	p.u.	p.u.	p.u.	p.u.	p.u.	p.u.	p.u.	

In simplified approaches, such a permutation can also be ignored and one calculates the number of reconfigured PV panels for the reconfigured solution. For simplicity, let us assume that the first one $l = 1$ corresponds to the reconfigured solution without row permutation, all other T_{st}^l can be calculated similarly.

$$T_{st}^1 = \sum_{i=1}^m |A'_i \setminus A_i| \quad (9)$$

where $|.|$ means the number of elements of a set (i.e. the potential of a set), set A_i is defined as the set of panels in the i -th row, i.e. the set $\{n * (i-1) + 1, n * (i-1) + 2, \dots, n * (i-1) + n\}$; A'_i is the set of reconstructed panels consisting of the images of elements in A_i mapped by the reconstruction solution, i.e. $A'_i = \{f(n * (i-1) + 1), f(n * (i-1) + 2), \dots, f(n * (i-1) + n)\}$; A'_i / A_i means to find the set of elements in A'_i but not in A_i .

III. MODELLING THE COST OF RECONFIGURATION

After the aging map of a PV array is detected, a remedial measure can be employed to rearrange the faulted PV modules, prior to the replacement of the faulted modules which increases the capital cost. For large-scale PV arrays, there are many reconfiguration routes. Different routes have different line reconnection time and wiring distances that determine the efficiency and cost of the reconfiguration progress.

In order to propose an optimised reconfiguration solution, it is necessary to model the reconfiguration cost, which is approximated by the number of reconfigured panels for simplicity.

A. CALCULATION OF PERMUTATION NUMBER BASED ON BRANCH AND BOUND METHOD

Branch-and-Bound (B&B) algorithm is one of the fundamental schemes for the combinatorial search problems. It has been widely applied to NP-hard optimization problems such as intelligent system design, integer programming, SAT problems, and theorem proving. Many researches concerning the theory and application of B&B have been reported in the literature. B&B has four basic components: the rules of branching, selection rules, selection rules and termination conditions. Branch rules and termination conditions depend on the specific search problem, and the selection rules referring to the slipknot point to identify the table has a better one or more nodes in order to further expand, elimination rules for as much as possible will not be able to derive the optimal solution of a node set to promulgate the point. The PV array module calculated by GA should be switched on and off again, and the minimum number of replacements is required.

It is shown in Figure 3 that the PV array switch replacement belongs to a wiring problem. Its solution space is a graph, so it is used as the first extended node from the starting position a.

TABLE 4. PV array before arrangement for second case in UK.

Before																			
0.7	0.8	0.7	0.5	0.4	0.8	0.5	0.7	0.4	0.4	0.7	0.8	0.7	0.5	0.4	0.8	0.5	0.7	0.4	0.3
p.u.	p.u.	p.u.	p.u.	p.u.	p.u.	p.u.	p.u.	p.u.	p.u.	p.u.	p.u.	p.u.	p.u.	p.u.	p.u.	p.u.	p.u.	p.u.	p.u.
0.6	0.7	0.6	0.7	0.7	0.7	0.4	0.7	0.6	0.6	0.6	0.7	0.6	0.7	0.7	0.7	0.4	0.7	0.6	0.6
p.u.	p.u.	p.u.	p.u.	p.u.	p.u.	p.u.	p.u.	p.u.	p.u.	p.u.	p.u.	p.u.	p.u.	p.u.	p.u.	p.u.	p.u.	p.u.	p.u.
0.7	0.7	0.7	0.8	0.6	0.6	0.8	0.5	0.7	0.6	0.7	0.7	0.7	0.8	0.6	0.6	0.8	0.5	0.7	0.6
p.u.	p.u.	p.u.	p.u.	p.u.	p.u.	p.u.	p.u.	p.u.	p.u.	p.u.	p.u.	p.u.	p.u.	p.u.	p.u.	p.u.	p.u.	p.u.	p.u.
0.8	0.6	0.7	0.7	0.6	0.7	0.7	0.8	0.5	0.5	0.8	0.6	0.7	0.7	0.7	0.7	0.7	0.8	0.5	0.7
p.u.	p.u.	p.u.	p.u.	p.u.	p.u.	p.u.	p.u.	p.u.	p.u.	p.u.	p.u.	p.u.	p.u.	p.u.	p.u.	p.u.	p.u.	p.u.	p.u.
0.8	0.8	0.8	0.6	0.5	0.5	0.7	0.5	0.6	0.5	0.8	0.8	0.7	0.6	0.5	0.5	0.7	0.5	0.6	0.5
p.u.	p.u.	p.u.	p.u.	p.u.	p.u.	p.u.	p.u.	p.u.	p.u.	p.u.	p.u.	p.u.	p.u.	p.u.	p.u.	p.u.	p.u.	p.u.	p.u.
0.7	0.9	0.8	0.7	0.6	0.5	0.6	0.9	0.7	0.5	0.7	0.9	0.8	0.7	0.6	0.5	0.6	0.9	0.7	0.5
p.u.	p.u.	p.u.	p.u.	p.u.	p.u.	p.u.	p.u.	p.u.	p.u.	p.u.	p.u.	p.u.	p.u.	p.u.	p.u.	p.u.	p.u.	p.u.	p.u.
0.9	0.9	0.8	0.7	0.6	0.6	0.6	0.9	0.7	0.9	0.7	0.8	0.8	0.7	0.9	0.6	0.6	0.9	0.8	0.7
p.u.	p.u.	p.u.	p.u.	p.u.	p.u.	p.u.	p.u.	p.u.	p.u.	p.u.	p.u.	p.u.	p.u.	p.u.	p.u.	p.u.	p.u.	p.u.	p.u.
After																			
0.6	0.6	0.8	0.5	0.5	0.5	0.5	0.5	0.5	0.5	0.5	0.5	0.5	0.5	0.5	0.5	0.5	0.4	0.3	
p.u.	p.u.	p.u.	p.u.	p.u.	p.u.	p.u.	p.u.	p.u.	p.u.	p.u.	p.u.	p.u.	p.u.	p.u.	p.u.	p.u.	p.u.	p.u.	p.u.
0.9	0.6	0.6	0.7	0.8	0.8	0.8	0.7	0.8	0.8	0.7	0.8	0.8	0.8	0.7	0.7	0.7	0.5	0.5	
p.u.	p.u.	p.u.	p.u.	p.u.	p.u.	p.u.	p.u.	p.u.	p.u.	p.u.	p.u.	p.u.	p.u.	p.u.	p.u.	p.u.	p.u.	p.u.	p.u.
0.7	0.7	0.8	0.7	0.7	0.7	0.8	0.7	0.7	0.8	0.7	0.7	0.7	0.7	0.7	0.7	0.7	0.5	0.5	
p.u.	p.u.	p.u.	p.u.	p.u.	p.u.	p.u.	p.u.	p.u.	p.u.	p.u.	p.u.	p.u.	p.u.	p.u.	p.u.	p.u.	p.u.	p.u.	p.u.
0.7	0.7	0.7	0.7	0.7	0.7	0.7	0.7	0.7	0.7	0.7	0.7	0.7	0.7	0.7	0.7	0.7	0.5	0.4	
p.u.	p.u.	p.u.	p.u.	p.u.	p.u.	p.u.	p.u.	p.u.	p.u.	p.u.	p.u.	p.u.	p.u.	p.u.	p.u.	p.u.	p.u.	p.u.	p.u.
0.7	0.7	0.7	0.7	0.7	0.7	0.7	0.6	0.7	0.6	0.6	0.6	0.6	0.6	0.6	0.6	0.6	0.6	0.4	
p.u.	p.u.	p.u.	p.u.	p.u.	p.u.	p.u.	p.u.	p.u.	p.u.	p.u.	p.u.	p.u.	p.u.	p.u.	p.u.	p.u.	p.u.	p.u.	p.u.
0.6	0.6	0.6	0.6	0.6	0.6	0.6	0.7	0.6	0.8	0.6	0.6	0.6	0.6	0.6	0.6	0.6	0.4	0.4	
p.u.	p.u.	p.u.	p.u.	p.u.	p.u.	p.u.	p.u.	p.u.	p.u.	p.u.	p.u.	p.u.	p.u.	p.u.	p.u.	p.u.	p.u.	p.u.	p.u.
0.8	0.9	0.9	0.9	0.9	0.9	0.9	0.9	0.9	0.9	0.8	0.8	0.8	0.8	0.8	0.8	0.8	0.5	0.4	
p.u.	p.u.	p.u.	p.u.	p.u.	p.u.	p.u.	p.u.	p.u.	p.u.	p.u.	p.u.	p.u.	p.u.	p.u.	p.u.	p.u.	p.u.	p.u.	p.u.

The feasible nodes adjacent to and accessible to the extended node are added to the queue of the node, and these squares are marked as 1, that is, the distance from the starting position a to these modules is 1. Then, the first node is taken from the node queue as the next extension node, and the unmarked position adjacent to the current extension node is marked as 2 and stored in the node queue. This process continues until the algorithm searches until the target location b or the queue at the node is empty. Then, a and b are interchanged with each other.

The specific algorithm is described as follows:

Step1: If the goal of the problem is to minimize, the value Z=infinity of the optimal solution is set.

Step2: According to the branching rule, a node from a Fathomed node (local solution) is selected and divided into several new nodes in the next level.

Step3: Calculate the lower bound for each newly branched node.

Step4: The insight condition is tested for each node. If the node satisfies any of the following conditions, the node can be known and will not be considered: the lower bound of the node is greater than or equal to the Z value. A feasible solution with minimum lower bound value has been found in this node. If this condition is true, it is necessary to compare the feasible solution with the z-value; if the former is small, it is necessary to update the z-value, which is the value of the feasible solution. This node cannot contain a viable solution.

Step5: To determine whether there are still unrecognized nodes. If unrecognized nodes exist, then proceed to step 2. If there are no unrecognized nodes, the calculation stops and the optimal solution is obtained.

Given any PV array with maximum power generation P_b before reconfiguration, denote P_a the maximum power generation after the above B&B reconfiguration, then there exists a functional relationship F to represent this B&B process.

$$P_a = F(P_b) \quad (10)$$

The corresponding flowchart is presented in Figure 4.

B. COST ANALYSIS OF PV ARRAY RECONSTRUCTION

According to the survey, it is assumed that the PV array needs to be reconstructed once a year on average and the PV array can generate power 8 hours per day. A skilled grid worker needs averagely 45 mins to swap the PV modules from one place to another. Through the reconstruction of PV array, the economic benefit of power generation can be increased minus the labor cost caused by handling. The following equations are employed to calculate the labor cost and the electricity profit. In (11), M_p is the pure profit of the reconfiguration. In (12), M_1 is the labor cost, T_{st} is the number of reconfigured PV panels, and M_s is the average salary of the manpower. In (13), M_2 is the additional electric revenue profit, P_a is the PV array output power after reconstruction, P_b is the PV array output power before reconstruction,

TABLE 5. PV array before arrangement for second case in turkey.

Before																								
0.7	0.8	0.7	0.5	0.4	0.8	0.5	0.7	0.4	0.4	0.7	0.8	0.7	0.7	0.5	0.4	0.8	0.5	0.7	0.4	0.4	0.3			
p.u.	p.u.	p.u.	p.u.	p.u.	p.u.	p.u.	p.u.	p.u.	p.u.	p.u.	p.u.	p.u.	p.u.	p.u.	p.u.	p.u.	p.u.	p.u.	p.u.	p.u.	p.u.	p.u.		
0.6	0.7	0.6	0.7	0.7	0.7	0.4	0.7	0.6	0.6	0.6	0.7	0.6	0.7	0.7	0.7	0.7	0.7	0.4	0.7	0.6	0.6	0.6		
p.u.	p.u.	p.u.	p.u.	p.u.	p.u.	p.u.	p.u.	p.u.	p.u.	p.u.	p.u.	p.u.	p.u.	p.u.	p.u.	p.u.	p.u.	p.u.	p.u.	p.u.	p.u.	p.u.		
0.7	0.7	0.7	0.8	0.6	0.6	0.8	0.5	0.7	0.6	0.7	0.7	0.7	0.8	0.6	0.6	0.8	0.5	0.7	0.6	0.6	0.6	0.6		
p.u.	p.u.	p.u.	p.u.	p.u.	p.u.	p.u.	p.u.	p.u.	p.u.	p.u.	p.u.	p.u.	p.u.	p.u.	p.u.	p.u.	p.u.	p.u.	p.u.	p.u.	p.u.	p.u.		
0.8	0.6	0.7	0.7	0.6	0.7	0.7	0.8	0.5	0.5	0.8	0.6	0.7	0.7	0.7	0.7	0.7	0.7	0.7	0.8	0.5	0.7	0.7		
p.u.	p.u.	p.u.	p.u.	p.u.	p.u.	p.u.	p.u.	p.u.	p.u.	p.u.	p.u.	p.u.	p.u.	p.u.	p.u.	p.u.	p.u.	p.u.	p.u.	p.u.	p.u.	p.u.		
0.8	0.8	0.6	0.5	0.5	0.7	0.5	0.6	0.5	0.5	0.8	0.8	0.7	0.6	0.5	0.5	0.7	0.5	0.6	0.5	0.5	0.6	0.5		
p.u.	p.u.	p.u.	p.u.	p.u.	p.u.	p.u.	p.u.	p.u.	p.u.	p.u.	p.u.	p.u.	p.u.	p.u.	p.u.	p.u.	p.u.	p.u.	p.u.	p.u.	p.u.	p.u.		
0.7	0.9	0.8	0.7	0.6	0.5	0.6	0.9	0.7	0.5	0.7	0.9	0.8	0.7	0.6	0.5	0.6	0.9	0.7	0.5	0.7	0.5	0.5		
p.u.	p.u.	p.u.	p.u.	p.u.	p.u.	p.u.	p.u.	p.u.	p.u.	p.u.	p.u.	p.u.	p.u.	p.u.	p.u.	p.u.	p.u.	p.u.	p.u.	p.u.	p.u.	p.u.		
0.9	0.9	0.8	0.7	0.6	0.6	0.6	0.9	0.7	0.9	0.7	0.7	0.8	0.8	0.7	0.9	0.6	0.6	0.9	0.8	0.7	0.9	0.8		
p.u.	p.u.	p.u.	p.u.	p.u.	p.u.	p.u.	p.u.	p.u.	p.u.	p.u.	p.u.	p.u.	p.u.	p.u.	p.u.	p.u.	p.u.	p.u.	p.u.	p.u.	p.u.	p.u.		
After																								
0.6	0.6	0.6	0.5	0.5	0.5	0.5	0.5	0.5	0.5	0.5	0.5	0.5	0.5	0.5	0.5	0.5	0.5	0.5	0.4	0.3				
p.u.	p.u.	p.u.	p.u.	p.u.	p.u.	p.u.	p.u.	p.u.	p.u.	p.u.	p.u.	p.u.	p.u.	p.u.	p.u.	p.u.	p.u.	p.u.	p.u.	p.u.	p.u.	p.u.		
0.7	0.7	0.7	0.7	0.7	0.7	0.7	0.7	0.7	0.7	0.7	0.7	0.7	0.7	0.7	0.7	0.7	0.7	0.7	0.7	0.7	0.5	0.5		
p.u.	p.u.	p.u.	p.u.	p.u.	p.u.	p.u.	p.u.	p.u.	p.u.	p.u.	p.u.	p.u.	p.u.	p.u.	p.u.	p.u.	p.u.	p.u.	p.u.	p.u.	p.u.	p.u.		
0.8	0.8	0.8	0.8	0.8	0.8	0.8	0.8	0.8	0.8	0.8	0.8	0.8	0.8	0.8	0.8	0.8	0.8	0.8	0.7	0.8	0.5	0.7		
p.u.	p.u.	p.u.	p.u.	p.u.	p.u.	p.u.	p.u.	p.u.	p.u.	p.u.	p.u.	p.u.	p.u.	p.u.	p.u.	p.u.	p.u.	p.u.	p.u.	p.u.	p.u.	p.u.		
0.7	0.7	0.7	0.7	0.7	0.7	0.7	0.7	0.7	0.7	0.7	0.7	0.7	0.7	0.7	0.7	0.7	0.7	0.7	0.7	0.7	0.4	0.4		
p.u.	p.u.	p.u.	p.u.	p.u.	p.u.	p.u.	p.u.	p.u.	p.u.	p.u.	p.u.	p.u.	p.u.	p.u.	p.u.	p.u.	p.u.	p.u.	p.u.	p.u.	p.u.	p.u.		
0.7	0.7	0.7	0.7	0.7	0.7	0.7	0.7	0.7	0.7	0.7	0.6	0.6	0.6	0.6	0.6	0.6	0.6	0.6	0.6	0.6	0.4	0.4		
p.u.	p.u.	p.u.	p.u.	p.u.	p.u.	p.u.	p.u.	p.u.	p.u.	p.u.	p.u.	p.u.	p.u.	p.u.	p.u.	p.u.	p.u.	p.u.	p.u.	p.u.	p.u.	p.u.		
0.7	0.7	0.7	0.7	0.7	0.7	0.7	0.7	0.7	0.7	0.7	0.7	0.7	0.7	0.7	0.7	0.7	0.7	0.7	0.7	0.7	0.7	0.7		
p.u.	p.u.	p.u.	p.u.	p.u.	p.u.	p.u.	p.u.	p.u.	p.u.	p.u.	p.u.	p.u.	p.u.	p.u.	p.u.	p.u.	p.u.	p.u.	p.u.	p.u.	p.u.	p.u.		
0.6	0.6	0.6	0.6	0.6	0.6	0.6	0.6	0.6	0.6	0.6	0.6	0.6	0.6	0.6	0.6	0.6	0.6	0.6	0.6	0.6	0.4	0.4		
p.u.	p.u.	p.u.	p.u.	p.u.	p.u.	p.u.	p.u.	p.u.	p.u.	p.u.	p.u.	p.u.	p.u.	p.u.	p.u.	p.u.	p.u.	p.u.	p.u.	p.u.	p.u.	p.u.		
0.9	0.9	0.8	0.9	0.9	0.9	0.9	0.9	0.9	0.9	0.9	0.9	0.9	0.9	0.9	0.9	0.9	0.9	0.9	0.8	0.9	0.5	0.5		
p.u.	p.u.	p.u.	p.u.	p.u.	p.u.	p.u.	p.u.	p.u.	p.u.	p.u.	p.u.	p.u.	p.u.	p.u.	p.u.	p.u.	p.u.	p.u.	p.u.	p.u.	p.u.	p.u.		

M_e is the electricity price. The target is to peruse the maximum value for the M_p .

$$\max M_p = M_2 - M_1 \quad (11)$$

$$\text{subject to: } M_1 = (T_{st}/5) * M_s \quad (12)$$

$$M_2 = M_e * (P_a - P_b) * 8 * 365/1000 \quad (13)$$

and equations (8)-(10).

IV. SIMULATION AND CASE STUDIES

Take 2019 as a benchmark. Taking China, the United States, the United Kingdom and Turkey as examples, it is verified whether the topology reconstruction method of PV array can truly obtain better economic benefits. The detailed information is shown as presented in Table 1.

To demonstrate the validity of the proposed algorithm, a number of PV arrays with different sizes will be evaluated on 7×20 PV arrays. A commercial 300W PV module is considered in the simulation. The maximum power outputs from these PV configurations, both before and after arrangements, are determined by employing a PV array model constructed in Python, which was employed to carry out the calculations and the corresponding computing times for a 7×20 PV array was arranged. Our experimental environment is as follows: Intel(R) Core (7M) i7-8565u CPU @ 1.80GHz / Windows 10 / 8 GB / 512gb SSD / UHD 620.

The maximum output power in a healthy module is set as 1 p.u. (STC), where standard test conditions represent 1000 W/m² irradiance at 25 °C module temperature. A typical large-scale non-uniform aging PV array is employed as a testing branch, which is presented in the up side in Table 2 ~ Table 6, in which each number stands for the maximum output power due to aging. In each string, PV modules are in series connection and all the strings are parallel connected, which is the typical connection method for commercial PV arrays. The down side of the Table 2 is the result of reconfiguration with the proposed algorithm considering the manpower cost and electricity price in China. The down side of the Table 3 is the result of reconfiguration with the proposed algorithm considering the manpower cost and electricity price in USA. The down side of the Table 4 is the result of reconfiguration with the proposed algorithm considering the manpower cost and electricity price in the UK. The down side of the Table 5 is the result of reconfiguration with the proposed algorithm considering the manpower cost and electricity price in Turkey. The down side of the Table 6 is the result of reconfiguration that only considers additional electric revenue profit.

Table 2 shows the simulation results that consider the electricity price and manpower cost in China, in which eighty manual swapping times are required. Without considering the maximum economy benefit, the additional electric

TABLE 6. PV array before arrangement for second case in GA.

Before																			
0.7	0.8	0.7	0.5	0.4	0.8	0.5	0.7	0.4	0.4	0.7	0.8	0.7	0.5	0.4	0.8	0.5	0.7	0.4	0.3
p.u.	p.u.	p.u.	p.u.	p.u.	p.u.	p.u.	p.u.	p.u.	p.u.	p.u.	p.u.	p.u.	p.u.	p.u.	p.u.	p.u.	p.u.	p.u.	p.u.
0.6	0.7	0.6	0.7	0.7	0.7	0.4	0.7	0.6	0.6	0.6	0.7	0.6	0.7	0.7	0.7	0.7	0.4	0.7	0.6
p.u.	p.u.	p.u.	p.u.	p.u.	p.u.	p.u.	p.u.	p.u.	p.u.	p.u.	p.u.	p.u.	p.u.	p.u.	p.u.	p.u.	p.u.	p.u.	p.u.
0.7	0.7	0.7	0.8	0.6	0.6	0.8	0.5	0.7	0.6	0.7	0.7	0.7	0.8	0.6	0.6	0.8	0.5	0.7	0.6
p.u.	p.u.	p.u.	p.u.	p.u.	p.u.	p.u.	p.u.	p.u.	p.u.	p.u.	p.u.	p.u.	p.u.	p.u.	p.u.	p.u.	p.u.	p.u.	p.u.
0.8	0.6	0.7	0.7	0.6	0.7	0.7	0.8	0.5	0.5	0.8	0.6	0.7	0.7	0.7	0.7	0.7	0.8	0.5	0.7
p.u.	p.u.	p.u.	p.u.	p.u.	p.u.	p.u.	p.u.	p.u.	p.u.	p.u.	p.u.	p.u.	p.u.	p.u.	p.u.	p.u.	p.u.	p.u.	p.u.
0.8	0.8	0.8	0.6	0.5	0.5	0.7	0.5	0.6	0.5	0.8	0.8	0.7	0.6	0.5	0.5	0.7	0.5	0.6	0.5
p.u.	p.u.	p.u.	p.u.	p.u.	p.u.	p.u.	p.u.	p.u.	p.u.	p.u.	p.u.	p.u.	p.u.	p.u.	p.u.	p.u.	p.u.	p.u.	p.u.
0.7	0.9	0.8	0.7	0.6	0.5	0.6	0.9	0.7	0.5	0.7	0.9	0.8	0.7	0.6	0.5	0.6	0.9	0.7	0.5
p.u.	p.u.	p.u.	p.u.	p.u.	p.u.	p.u.	p.u.	p.u.	p.u.	p.u.	p.u.	p.u.	p.u.	p.u.	p.u.	p.u.	p.u.	p.u.	p.u.
0.9	0.9	0.8	0.7	0.6	0.6	0.6	0.9	0.7	0.9	0.7	0.8	0.8	0.7	0.9	0.6	0.6	0.9	0.8	0.7
p.u.	p.u.	p.u.	p.u.	p.u.	p.u.	p.u.	p.u.	p.u.	p.u.	p.u.	p.u.	p.u.	p.u.	p.u.	p.u.	p.u.	p.u.	p.u.	p.u.
After																			
0.9	0.9	0.9	0.9	0.9	0.9	0.9	0.9	0.9	0.9	0.8	0.8	0.8	0.8	0.8	0.8	0.9	0.5	0.5	0.5
p.u.	p.u.	p.u.	p.u.	p.u.	p.u.	p.u.	p.u.	p.u.	p.u.	p.u.	p.u.	p.u.	p.u.	p.u.	p.u.	p.u.	p.u.	p.u.	p.u.
0.8	0.8	0.8	0.8	0.8	0.8	0.8	0.8	0.8	0.8	0.8	0.8	0.8	0.8	0.8	0.8	0.7	0.7	0.7	0.5
p.u.	p.u.	p.u.	p.u.	p.u.	p.u.	p.u.	p.u.	p.u.	p.u.	p.u.	p.u.	p.u.	p.u.	p.u.	p.u.	p.u.	p.u.	p.u.	p.u.
0.7	0.7	0.7	0.7	0.7	0.7	0.7	0.7	0.7	0.7	0.7	0.7	0.7	0.7	0.7	0.7	0.7	0.7	0.5	0.5
p.u.	p.u.	p.u.	p.u.	p.u.	p.u.	p.u.	p.u.	p.u.	p.u.	p.u.	p.u.	p.u.	p.u.	p.u.	p.u.	p.u.	p.u.	p.u.	p.u.
0.7	0.7	0.7	0.7	0.7	0.7	0.7	0.7	0.7	0.7	0.7	0.7	0.7	0.7	0.7	0.7	0.7	0.7	0.4	0.4
p.u.	p.u.	p.u.	p.u.	p.u.	p.u.	p.u.	p.u.	p.u.	p.u.	p.u.	p.u.	p.u.	p.u.	p.u.	p.u.	p.u.	p.u.	p.u.	p.u.
0.7	0.7	0.7	0.7	0.7	0.7	0.7	0.7	0.7	0.7	0.6	0.6	0.6	0.6	0.6	0.6	0.6	0.6	0.4	0.4
p.u.	p.u.	p.u.	p.u.	p.u.	p.u.	p.u.	p.u.	p.u.	p.u.	p.u.	p.u.	p.u.	p.u.	p.u.	p.u.	p.u.	p.u.	p.u.	p.u.
0.6	0.6	0.6	0.6	0.6	0.6	0.6	0.6	0.6	0.6	0.6	0.6	0.6	0.6	0.6	0.6	0.6	0.6	0.4	0.4
p.u.	p.u.	p.u.	p.u.	p.u.	p.u.	p.u.	p.u.	p.u.	p.u.	p.u.	p.u.	p.u.	p.u.	p.u.	p.u.	p.u.	p.u.	p.u.	p.u.
0.6	0.6	0.6	0.5	0.5	0.5	0.5	0.5	0.5	0.5	0.5	0.5	0.5	0.5	0.5	0.5	0.5	0.5	0.4	0.3
p.u.	p.u.	p.u.	p.u.	p.u.	p.u.	p.u.	p.u.	p.u.	p.u.	p.u.	p.u.	p.u.	p.u.	p.u.	p.u.	p.u.	p.u.	p.u.	p.u.

revenue profit (M_2) is \$1192.06, and the corresponding labor cost (M_1) is \$693.75. When considering the maximum economy benefit, the additional electric revenue profit (M_2) is \$1059.61, the corresponding labor cost (M_1) is \$ 330. Comparing those two reconfigurations, although the additional electric revenue profit is decreased by 11.1% in the proposed method, the labor cost (M_1) is decreased by 52.4%, and the pure profit of the offline maintenance is increased by 46.4% due to the lower labor cost.

Table 3 displays the simulation results that consider the electricity price and manpower cost in USA, in which eighty manual swapping times are required. Without considering the maximum economy benefit, the additional electric revenue profit (M_2) is \$1773.90, and the corresponding labor cost (M_1) is \$ 1500.00. It is clear that the additional electric revenue profit and labor cost are higher than that in China due to the high electricity price and labor cost. When considering the maximum economy benefit, the additional electric revenue profit (M_2) is \$1379.70, the corresponding labor cost (M_1) is \$600. Comparing those two reconfigurations, although the additional electric revenue profit is decreased by 22.2% in the proposed method, the labor cost (M_1) is decreased by 60%, and the pure profit of the offline maintenance is increased by 191.9% due to the lower labor cost.

UK case is similar with the USA in electrify price and labor cost. Table 4 is the simulation results that consider

the electricity price and manpower cost in UK, in which eighty manual swapping times are required. Without considering the maximum economy benefit, the additional electric revenue profit (M_2) is \$3632.95, the corresponding labor cost (M_1) is \$1612.50. It is clear that the additional electric revenue profit and labor cost are higher than China due to the high electricity price and labor cost. With considering the maximum economy benefit, the additional electric revenue profit (M_2) is \$3229.29, the corresponding labor cost (M_1) is \$709.50. Comparing those two reconfigurations, although the additional electric revenue profit is decreased by 11% in the proposed method, the labor cost (M_1) is decreased by 56%, and the pure profit of the offline maintained is increased by 24.7% due to the lower labor cost.

Table 5 is the simulation results that consider the electricity price and manpower cost in Turkey, in which eighty manual swapping times are required. Without considering the maximum economy benefit, the additional electric revenue profit (M_2) is \$2412.50, the corresponding labor cost (M_1) is \$ 282.50. With considering the maximum economy benefit, the additional electric revenue profit (M_2) is \$2375.50, the corresponding labor cost (M_1) is \$ 213.75. Comparing those two reconfigurations, although the additional electric revenue profit is decreased by 1.5% in the proposed method, the labor cost (M_1) is decreased by 24%, and the pure profit of the offline maintained is increased by 1.4% due to the lower

labor cost. Due to the low cost of the manpower in Turkey and high electricity price, the proposed method can only improve 1.4% economy benefit by the proposed method.

According to the calculation from Table 7 and Table 8, in high manpower cost and low electricity price countries, the proposed algorithm can decrease the cost of the offline reconfiguration by decreasing the swapping times, and the total profit can be increased dramatically. In low manpower cost and high electricity price countries, although the proposed algorithm can decrease the cost of the manpower, the corresponding additional electric revenue profit is decreased as well; there is no clear profit increment.

TABLE 7. Economic benefit analysis considering the minimum handling times.

Country	$M_2(\$)$	$M_I(\$)$	$M_p(\$)$
China	1059.61	330.00	729.61
USA	1379.70	600.00	779.70
UK	3229.29	709.50	2520.10
Turkey	2375.50	213.75	2161.75

TABLE 8. Economic benefit analysis without considering the minimum handling times.

Country	$M_2 (\$)$	$M_I (\$)$	$M_p (\$)$
China	1192.06	693.75	498.31
USA	1773.90	1500.00	273.90
UK	3632.95	1612.50	2020.45
Turkey	2412.50	282.50	2130.00

V. CONCLUSION

Non-uniform aging of PV modules is a long-lasting challenge for large large-scale PV arrays, which not only decrease the output power of the PV array, but also damage the PV modules if left untreated. Without rearranging non-uniformly aged PV arrays, typical online global-MPPT schemes can only track a compromised maximum rather than its potential maximum power of the Non-uniform aging of PV array. This paper has proposed a new PV array reconfiguration strategy considering the lowest cost of manpower and electricity price. The manpower cost and electricity price in USA, China, UK and Turkey are considered in the paper to investigate the different reconfigurations. A 7×20 array is employed to verify the proposed reconfirmation algorithm. Due to the difference of the manpower and electrify price in different countries, for the same non-uniform aging 7×20 PV array, there is about 46.4% increment in the profit for the in China application scenario in China; there is about 191.9% increment in profit in USA application scenario; there is about 24.7% profit in UK application scenario; there is about 1.4% increment in profit in Turkey application scenario. The proposed method also could be used in other countries to maintain the aged PV arrays. For the high electricity price and low labor cost countries, such as South Africa, Turkey, etc., the proposed algorithm may not have clear profit increment. The proposed algorithm will give more finical increment in the low electricity price and high labor cost countries, such as USA, UK, Saudi Arabia

REFERENCES

- [1] P. L. Carotenuto, P. Manganiello, G. Petrone, and G. Spagnuolo, "Online recording a PV module fingerprint," *IEEE J. Photovolt.*, vol. 4, no. 2, pp. 659–668, Mar. 2014.
- [2] Y. A. Mahmoud, W. Xiao, and H. H. Zeineldin, "A parameterization approach for enhancing PV model accuracy," *IEEE Trans. Ind. Electron.*, vol. 60, no. 12, pp. 5708–5716, Dec. 2013.
- [3] Y. Hu, W. Cao, J. Ma, S. J. Finney, and D. Li, "Identifying PV module mismatch faults by a thermography-based temperature distribution analysis," *IEEE Trans. Device Mater. Rel.*, vol. 14, no. 4, pp. 951–960, Dec. 2014.
- [4] M. Z. Shams El-Dein, M. Kazerani, and M. M. A. Salama, "Optimal photovoltaic array reconfiguration to reduce partial shading losses," *IEEE Trans. Sustain. Energy*, vol. 4, no. 1, pp. 145–153, Jan. 2013.
- [5] M. Mattei, G. Notton, C. Cristofari, M. Muselli, and P. Poggi, "Calculation of the polycrystalline PV module temperature using a simple method of energy balance," *Renew. Energy*, vol. 31, no. 4, pp. 553–567, Apr. 2006.
- [6] M. Boztepe, F. Guinjoan, G. Velasco-Quesada, S. Silvestre, A. Chouder, and E. Karatepe, "Global MPPT scheme for photovoltaic string inverters based on restricted voltage window search algorithm," *IEEE Trans. Ind. Electron.*, vol. 61, no. 7, pp. 3302–3312, Jul. 2014.
- [7] M. Abdelhamid, R. Singh, and M. Omar, "Review of microcrack detection techniques for silicon solar cells," *IEEE J. Photovolt.*, vol. 4, no. 1, pp. 514–524, Jan. 2014.
- [8] B. N. Alajmi, K. H. Ahmed, S. J. Finney, and B. W. Williams, "A maximum power point tracking technique for partially shaded photovoltaic systems in microgrids," *IEEE Trans. Ind. Electron.*, vol. 60, no. 4, pp. 1596–1606, Apr. 2013.
- [9] *Produce Information, Yingli Solar Ltd.* Accessed: 2018. [Online]. Available: <http://www.yinglisolar.com/en/products/solar-modules/>
- [10] Y. Hu, Y. Deng, Q. Liu, and X. He, "Asymmetry three-level gird-connected current hysteresis control with varying bus voltage and virtual oversample method," *IEEE Trans. Power Electron.*, vol. 29, no. 6, pp. 3214–3222, Jun. 2014.
- [11] B. Zhao, Q. Song, W. Liu, and Y. Sun, "A synthetic discrete design methodology of high-frequency isolated bidirectional DC/DC converter for grid-connected battery energy storage system using advanced components," *IEEE Trans. Ind. Electron.*, vol. 61, no. 10, pp. 5402–5410, Oct. 2014.
- [12] W. Li, W. Li, X. Xiang, Y. Hu, and X. He, "High step-up interleaved converter with built-in transformer voltage multiplier cells for sustainable energy applications," *IEEE Trans. Power Electron.*, vol. 29, no. 6, pp. 2829–2836, Jun. 2014.
- [13] S. Djordjevic, D. Parlevliet, and P. Jennings, "Detectable faults on recently installed solar modules in western australia," *Renew. Energy*, vol. 67, pp. 215–221, Jul. 2014.
- [14] E. L. Meyer and E. E. van Dyk, "Assessing the reliability and degradation of photovoltaic module performance parameters," *IEEE Trans. Rel.*, vol. 53, no. 1, pp. 83–92, Mar. 2004.
- [15] E. V. Paraskevadaki and S. A. Papathanassiou, "Evaluation of MPP voltage and power of mc-Si PV modules in partial shading conditions," *IEEE Trans. Energy Convers.*, vol. 26, no. 3, pp. 923–932, Sep. 2011.
- [16] C. Buerhop, D. Schlegel, M. Niess, C. Vodermayer, R. Weißmann, and C. J. Brabec, "Reliability of IR-imaging of PV-plants under operating conditions," *Sol. Energy Mater. Sol. Cells*, vol. 107, pp. 154–164, Dec. 2012.
- [17] Y. Hu, B. Gao, X. Song, G. Y. Tian, K. Li, and X. He, "Photovoltaic fault detection using a parameter based model," *Sol. Energy*, vol. 96, pp. 96–102, Oct. 2013.
- [18] Z. Zou, Y. Hu, B. Gao, W. L. Woo, and X. Zhao, "Study of the gradual change phenomenon in the infrared image when monitoring photovoltaic array," *J. Appl. Phys.*, vol. 115, no. 4, pp. 1–11, 2014.
- [19] M. Simon and E. L. Meyer, "Detection and analysis of hot-spot formation in solar cells," *Sol. Energy Mater. Sol. Cells*, vol. 94, no. 2, pp. 106–113, Feb. 2010.
- [20] J. Kurnik, M. Jankovec, K. Brecl, and M. Topic, "Outdoor testing of PV module temperature and performance under different mounting and operational conditions," *Sol. Energy Mater. Sol. Cells*, vol. 95, no. 1, pp. 373–376, Jan. 2011.
- [21] Y. Hu, W. Cao, J. Wu, B. Ji, and D. Holliday, "Thermography-based virtual MPPT scheme for improving PV energy efficiency under partial shading conditions," *IEEE Trans. Power Electron.*, vol. 29, no. 11, pp. 5667–5672, Nov. 2014.

- [22] T. Takashima, J. Yamaguchi, K. Otani, T. Oozeki, K. Kato, and M. Ishida, "Experimental studies of fault location in PV module strings," *Sol. Energy Mater. Sol. Cells*, vol. 93, nos. 6–7, pp. 1079–1082, Jun. 2009.
- [23] R. A. Kumar, M. S. Suresh, and J. Nagaraju, "Measurement of AC parameters of gallium arsenide (GaAs/Ge) solar cell by impedance spectroscopy," *IEEE Trans. Electron Devices*, vol. 48, no. 9, pp. 2177–2179, Sep. 2001.
- [24] A. Chouder and S. Silvestre, "Automatic supervision and fault detection of PV systems based on power losses analysis," *Energy Convers. Manage.*, vol. 51, no. 10, pp. 1929–1937, Oct. 2010.
- [25] S. Silvestre, A. Chouder, and E. Karatepe, "Automatic fault detection in grid connected PV systems," *Sol. Energy*, vol. 94, pp. 119–127, Aug. 2013.
- [26] D. Nguyen and B. Lehman, "An adaptive solar photovoltaic array using model-based reconfiguration algorithm," *IEEE Trans. Ind. Electron.*, vol. 55, no. 7, pp. 2644–2654, Jul. 2008.
- [27] J. P. Storey, P. R. Wilson, and D. Bagnall, "Improved optimization strategy for irradiance equalization in dynamic photovoltaic arrays," *IEEE Trans. Power Electron.*, vol. 28, no. 6, pp. 2946–2956, Jun. 2013.
- [28] J. Storey, P. R. Wilson, and D. Bagnall, "The optimized-string dynamic photovoltaic array," *IEEE Trans. Power Electron.*, vol. 29, no. 4, pp. 1768–1776, Apr. 2014.
- [29] Y. Wang, X. Lin, Y. Kim, N. Chang, and M. Pedram, "Architecture and control algorithms for combating partial shading in photovoltaic systems," *IEEE Trans. Comput.-Aided Design Integr. Circuits Syst.*, vol. 33, no. 6, pp. 917–929, Jun. 2014.
- [30] G. Velasco-Quesada, F. Guinjoan-Gispert, R. Pique-Lopez, M. Roman-Lumbrales, and A. Conesa-Roca, "Electrical PV array reconfiguration strategy for energy extraction improvement in grid-connected PV systems," *IEEE Trans. Ind. Electron.*, vol. 56, no. 11, pp. 4319–4331, Nov. 2009.
- [31] A. Ndiaye, C. M. F. Kébé, A. Charki, P. A. Ndiaye, V. Sambou, and A. Kobi, "Degradation evaluation of crystalline-silicon photovoltaic modules after a few operation years in a tropical environment," *Sol. Energy*, vol. 103, pp. 70–77, May 2014.
- [32] C. R. Osterwald, A. Anderberg, S. Rummel, and L. Ottoson, "Degradation analysis of weathered crystalline-silicon PV modules," in *Proc. Conf. Rec. 29th IEEE Photovoltaic Spec. Conf.*, May. 2002, pp. 1392–1395.
- [33] L. Cristaldi, M. Faifer, M. Rossi, S. Toscani, M. Catelani, L. Ciani, and M. Lazzaroni, "Simplified method for evaluating the effects of dust and aging on photovoltaic panels," *Measurement*, vol. 54, pp. 207–214, Aug. 2014.
- [34] A. Ndiaye, C. M. F. Kébé, P. A. Ndiaye, A. Charki, A. Kobi, and V. Sambou, "A novel method for investigating photovoltaic module degradation," *Energy Procedia*, vol. 36, pp. 1222–1231, 2013.
- [35] M. A. Munoz, M. C. Alonso-García, N. Vela, and F. Chenlo, "Early degradation of silicon PV modules and warranty conditions," *Sol. Energy*, vol. 85, no. 9, pp. 2264–2274, Sep. 2011.
- [36] D. Chianese, N. Cereghetti, S. Rezzonico, and G. Travaglini, "18 types of PV modules under the lens," in *Proc. 16th Euro. PV Sol. Energy Conf.*, Glasgow, Scotland, May 2000, pp. 1–4.



CHEN ZHANG received the M.S. degree in computer science from the China University of Mining and Technology, in 2004, and the Ph.D. degree in computer application technology from the China University of Mining and Technology, in 2014. She is currently a Lecturer with the School of Computer Science and Technology, CUMT. Her research interest is computer science. Her interest is focused on using computational intelligence and machine-learning techniques to find potential modalities and patterns from the massive data of power systems.



MOHAMMED ALKAHTANI was born in Arar, Saudi Arabia. He received the B.Eng. degree (Hons.) in electrical and electronics engineering, and the M.Sc. degree in electrical power and control engineering from Liverpool John Moores University, Liverpool, U.K., in 2014 and 2016, respectively. He is currently pursuing the Ph.D. degree with the University of Liverpool. His research interests include soiling management of photovoltaic and a PV array efficiency improvement.



YIHUA HU (Senior Member, IEEE) received the B.S. degree in electrical motor drives, and the Ph.D. degree in power electronics and drives from the China University of Mining and Technology, in 2003 and 2011, respectively. Between 2011 and 2013, he was with the College of Electrical Engineering, Zhejiang University, as a Postdoctoral Fellow. Between 2013 and 2015, he worked as a Research Associate with the Power Electronics and Motor Drive Group, University of Strathclyde. He is currently a Lecturer with the Department of Electrical Engineering and Electronics, University of Liverpool (UoL). He has published 65 articles in IEEE TRANSACTIONS journals. His research interests include renewable generation, power electronics converters and control, electric vehicle, more electric ship/aircraft, smart energy system, and nondestructive test technology. He is also an Associate Editor of *IET Renewable Power Generation*, *IET Intelligent Transport Systems*, and *Power Electronics and Drives*.



JIANGFENG ZHANG received the B.Sc. and Ph.D. degrees in mathematics from Xi'an Jiaotong University, and the Ph.D. degree in electronic and electrical engineering from the University of Strathclyde.

He was a Lecturer with the Shanghai Jiaotong University from 2000 to 2002, then a Postdoctoral Researcher in a number of universities before he moved to the University of Pretoria, in 2006, where he was appointed as a Research Fellow, a Senior Lecturer, and eventually an Associate Professor. He moved to the University of Strathclyde, in 2013, and then the University of Technology Sydney, in 2016. He joined the Department of Automotive Engineering, Clemson University, in October 2019. His current research interests are electric vehicle related topics, ranging from battery management, smart grid, renewable energy, energy efficiency, and demand side management (DSM). His research experience includes electric vehicle battery charging/discharging control and grid integration, peer-to-peer energy trading, electricity market, distributed generation planning, solar thermal and PV efficiency, electric power dispatch, generator maintenance scheduling, operational efficiency improvement of industrial energy systems (pumps, conveyors, winders, and crushers), residential demand response, measurement and verification, building energy audit, and nonlinear control systems amongst others.

Dr. Zhang is currently a Fellow of IET, a member of the IFAC TC6.3 (power and energy systems), a Chartered Engineer (registered with the IET), and an Associate Editor of *IET Renewable Power Generation* and *IET Smart Grid*.



ZUYU WU was born in Shannxi, China, in December 5, 1990. He received the B.Eng. and M.Eng. degrees in electrical engineering from Newcastle University, Newcastle, U.K., in 2015 and 2018, respectively. He is currently pursuing the Ph.D. degree with the University of York. His research interests include photovoltaics soiling management and MPPT of PV power generation.